# Disturbance performance comparison of predictive controllers in SCFs

**Maria Alice de F. Marques** [*] **Igor M. L. Pataro** [**]
**Marcus V. Americano da Costa** [***] **José D. Álvarez** [**]

[*] *Postgraduate Program in Mechatronics at the Federal University of Bahia, Salvador, BA-40210910, Brazil.*
[**] *University of Almería, CIESOL, ceiA3, Department of Informatics, 04120 Almería, Spain*
[***] *National Institute of Science and Technology in Control and Automation of Energy Processes, Department of Automation and Systems Engineering, Federal University of Santa Catarina, Florianópolis-SC, Brazil.*

**Abstract:** This study performs a comparative analysis between a linear and a non-linear predictive controller (MPC and NMPC, respectively) in controlling the output temperature of a solar thermal collector field (SCF), the main component that dictates the overall efficiency of the solar thermal plant. The controllers are evaluated using a validated non-linear model of a real solar plant facility located in the CIESOL center at the University of Almería, Spain. While the linear MPC is based on a linearized model implemented at a specific working point of the plant, the NMPC uses the full nonlinear dynamic model to predict the outlet temperature under similar conditions. The comparison considers the effect of the computational load of nonlinear controllers due to the nonlinear optimization problem, which can compromise disturbance rejection performance on cloudy days. Therefore, both controllers are explored in an ideal sunny day scenario as a benchmark result, and subsequently, the MPC and NMPC are evaluated in a critically cloudy scenario. The simulation results show that the controllers have similar behavior in both scenarios; however, the NMPC demonstrated to have lower control effort compared to the MPC in cloudy day scenarios. These findings offer insights for future applications of predictive controllers considering effectiveness and performance in disturbance rejection, which can culminate in improving the efficiency of SCFs.

*Keywords:* Predictive control, feedforward action, thermal solar energy, SCF, renewable energy.

## 1. INTRODUCTION

Reliance on non-renewable energy sources remains a key contributor to global warming, exacerbating environmental crises worldwide and requiring urgent renewable energy developments (Renewables Systems, 2024). Among several solutions, solar energy stands as an effective renewable energy to replace fossil-fuel sources in the global scenario. The use of solar energy can be used for power generation or heat power production, which contributes to reducing greenhouse gas emissions, mitigating climate change, and alleviating dependence on finite energy resources. However, increasing the efficiency of solar energy systems is crucial to catch its benefits and fully accelerate its widespread adoption.

In the realm of solar thermal energy, achieving efficiency requires precise control of the heat transfer fluid (HTF) within solar collector field (SCF) systems. In such systems, the control variable is the HTF outlet temperature, while the manipulated variable is the HTF flow rate, since the source energy (solar irradiance) cannot be directly adjusted. In addition, the HTF inlet temperature, ambient temperature, and irradiance itself are considered disturbances that challenge control, requiring accurate modeling of the system's nonlinear dynamics, robustness against uncertainties, and the complexity of balancing computational cost with response times to ensure optimal performance. Over the past 30 years, deep research has been done investigating advanced control strategies for solar thermal systems in order to obtain fine manipulation of the HTF outlet temperature (Camacho et al., 2012). Among them, Model Predictive Control (MPC) Camacho and Bordons (2017) stands out as an effective approach to optimize the efficiency and performance of SCF systems Camacho et al. (2007); Masero et al. (2022); Lemos (2006); Pataro et al. (2021, 2022). MPC is a control technique where the control action is determined by solving a finite horizon optimal control problem at each sampling instant. Only the first control action is implemented, while the remaining future inputs are discarded. This process is repeated continuously, updating predictions with new system measurements, in an approach known as the receding horizon technique.

Several works in the literature have addressed the concerns regarding MPC applied to SCF. For instance, the work of Navas et al. (2018) evaluates two strategies for controlling

distributed SCFs with the aim of maximizing electrical energy generation when receiving different degrees of solar radiation. Pintaldi et al. (2019) present a MPC based on a genetic algorithm to minimize reserve power consumption in SCF systems. In work of Gallego et al. (2022), an MPC is associated with two feedforwards (FF) control approaches in order to reject disturbances in the HTF pump flow of SCFs. In addition, MPC strategies are also discussed in Li et al. (2020), which analyzes the energy savings of water flow with adaptive control in a solar collector model. A comprehensive review of control strategies applied to SCF is presented by Camacho et al. (2007), in which the authors suggest that an advanced model-based approach with high-order controllers is recommended to control such systems, aiming to address the system nonlinearity and delays and provide precise control and acceptable disturbance rejection.

As discussed by Camacho et al. (2007), nonlinear MPC (NMPC) is highly indicated to face the challenges of controlling SCF due to its capabilities to match the system's nonlinear dynamic and consider optimal control action and the system constraints. Nevertheless, NMPC inherently presents a high computational cost, which is crucial to determining the sample time in which the controller is employed. On this concern, large sample times can compromise disturbance rejection since the system is constantly disturbed at moments when the controller may have no action. Hence, dealing with this compromise situation is mandatory when designing NMPC for SCFs.

Therefore, based on the previous commitment regarding NMPC strategies applied to the SCF, in this article we will address the application of MPC techniques in an SCF and compare the effectiveness of linear and explicitly nonlinear predictive strategies to analyze temperature regulation for day scenarios sunny and cloudy. The comparison seeks to expose results that can assist in decision-making in relation to thermal energy processes, depending on which resources and hardware structure are available for the control application. The main comparison is related to the performance of the NMPC, which, despite having its nominal model compatible with the system dynamics, may have reduced performance in cases of very strong irradiance disturbances due to the long computational and sampling time. In the case of MPC, the linear model is obtained for a specific operating point, and by obtaining a linear model, the optimization problem is much simpler and faster, which requires a shorter sampling time to calculate control actions. For this, the controllers will be analyzed under the same conditions in a simulation scenario considering real data for sunny and cloudy day situations using the nonlinear model of the CIESOL plant, located at the University of Almería, southern Spain, and compared in reference tracking and disturbance rejection scenarios.

This article is organized as follows: Section 2 describes the SCF model of the CIESOL thermal plant used as a test-bed system for simulation experiments. In Section 3, the MPC and NMPC are formulated in which a state space representation with an incremental form of the inputs is used for the output predictions of the linear MPC strategy while the validated nonlinear model is used to compute the output predictions within the NMPC. Section 4 presents the simulation results using real data of the actual facility and the validated nonlinear model of the CIESOL SCFs to emulate the actual system. Finally, the conclusions of the work are presented in Section 5.

## 2. SOLAR THERMAL COLLECTOR MODEL

The SCF model discussed in this article is part of a facility at the CIESOL center of the University of Almería, Spain. This integrated system is designed to maintain hot water for a charging system along with storage tanks and gas heaters. Figure 1 illustrates the CIESOL flat-plate collectors.

Figure 1. CIESOL thermal plant facility.

The SCF model is formulated as a simplified differential equation with lumped parameters, described in (1), such as

$$\rho \cdot C_p \cdot A_s f \cdot \frac{dT_{sc,o}(t)}{dt} = \beta \cdot I(t) - \frac{H}{L_{eq}} \cdot (T_{sc,m}(t) - T_a(t)) - \rho \cdot C_p \cdot \frac{q(t-d_q)}{c_f} \cdot \frac{(T_{sc,o}(t) - T_{sc,in}(t))}{L_{eq}} \quad (1)$$

where $\rho$ is the HTF density, $Cp$ is the specific heat capacity of water, $A_{sf}$ is the cross-sectional area of the solar collector tube, $\beta$ is the irradiance model parameter, $T_{sc,o}(t)$ and $T_{sc,in}(t)$ are the outlet and inlet temperatures of the SCF system, respectively, $I(t)$ and $T_a(t)$ are the solar irradiance and ambient temperature, respectively, and $H$ is the overall loss coefficient. $T_{sc,m}(t)$ is the average between the inlet and outlet temperatures, i.e., $T_{sc,m}(t) = (T_{sc,o}(t) + T_{sc,in}(t))/2$. Moreover, $L_{eq}$ is the equivalent length of the absorber tube considering an equivalent flow $q(t)$, and $c_f$ is the conversion factor to account for connections, number of modules, and $m^3$/s conversion. Moreover, the term $d_q$ is the time delay of the HTF flow related to the HTF output temperature. The validated parameter values used in this work are described in Table 1.

Aiming to develop the MPC strategy, it is necessary to linearize the plant model around a system operating point. For this, the linear approximation using the Taylor series expansions truncated in the first derivative is used, in which the deviation variable $\check{\mathbb{X}}(t) = \overline{\mathbb{X}} - \mathbb{X}(t)$ refers to

the increment of the variable in relation to the chosen equilibrium point $\overline{\mathbb{X}}$,

$$\begin{aligned}&\frac{\rho \cdot C_p \cdot A_{sf}}{\frac{\rho \cdot C_p \cdot \overline{q}}{c_f \cdot L_{eq}} + \frac{H}{2 \cdot L_{eq}}} \cdot \frac{d\check{T}_{sc,o}(t)}{dt} + \check{T}_{sc,o}(t) = \\ &\frac{-\frac{C_p \cdot \rho}{c_f \cdot L_{eq}} \cdot (\overline{T}_{sc,o} - \overline{T}_{sc,in})}{\frac{\rho \cdot C_p \cdot \overline{q}}{c_f \cdot L_{eq}} + \frac{H}{2 \cdot L_{eq}}} \cdot \check{q}(t - d_q) \\ &+ \frac{\beta}{\frac{\rho \cdot C_p \cdot \overline{q}}{c_f \cdot L_{eq}} + \frac{H}{2 \cdot L_{eq}}} \cdot I(t) + \frac{\frac{\rho \cdot C_p \cdot \overline{q}}{c_f \cdot L_{eq}} - \frac{H}{2 \cdot L_{eq}}}{\frac{\rho \cdot C_p \cdot \overline{q}}{c_f \cdot L_{eq}} + \frac{H}{2 \cdot L_{eq}}} \cdot \check{T}_{in}(t) \\ &+ \frac{\frac{H}{L_{eq}}}{\frac{\rho \cdot C_p \cdot \overline{q}}{c_f \cdot L_{eq}} + \frac{H}{2 \cdot L_{eq}}} \cdot \check{T}_a(t)\end{aligned} \quad . \tag{2}$$

Considering that the MPC implementation will be formulated in the space state form, and its variables defined in the next section, the transfer functions of (2) are derived regarding each system input, following the Laplace frequency domain $s$ transform, resulting in

$$\check{T}_{sc,o}(s) = \frac{K_I \check{I}(s) + K_{T_a} \check{T}_a(s) + K_{T_{in}} \check{T}_{in}(s) + K_q e^{-t_{d_q} s} \check{q}(s)}{(\tau s + 1)} \tag{3}$$

where the linear model parameters are defined as

$$\begin{aligned}K_q &= \frac{-\frac{C_p \rho}{c_f L}(\overline{T}_{sc,o} - \overline{T}_{sc,i})}{\left[\frac{\rho C_p \overline{q}}{c_f L_{eq}} + \frac{H}{2L_{eq}}\right]} \qquad K_I = \frac{\beta}{\left[\frac{\rho C_p \overline{q}}{c_f L_{eq}} + \frac{H}{2L_{eq}}\right]} \\ K_{T_{sc,in}} &= \frac{\left[\frac{\rho C_p \overline{q}}{c_f L_{eq}} - \frac{H}{2L_{eq}}\right]}{\left[\frac{\rho C_p \overline{q}}{c_f L_{eq}} + \frac{H}{2L_{eq}}\right]} \qquad K_{T_a} = \frac{\frac{H}{L}}{\left[\frac{\rho C_p \overline{q}}{c_f L_{eq}} + \frac{H}{2L_{eq}}\right]} \\ \tau &= \frac{\rho C_p A_{sc}}{\left[\frac{\rho C_p \overline{q}}{c_f L_{eq}} + \frac{H}{2L_{eq}}\right]}\end{aligned} \tag{4}$$

Following the proposed models, (1) and (4) are used to compute the output predictions for the MPC and NMPC detailed in the next section.

## 3. CONTROL METHODS

In this section, the MPC and NMPC optimization problems are presented to compute the optimal control actions for the SCF systems. On the one hand, the MPC state space model is used along with the incremental form of the inputs to include the artificial integrative pole to eliminate steady-state error. Moreover, the disturbances model is also considered, with the aim of including the FF action. On the other hand, the nonlinear model in (1) is used to compute the output predictions of the NMPC, in which it already included the disturbance dynamics explicitly.

Table 1. Description of the solar collector model parameters

| Parameter | Unit |
|---|---|
| $A_{sf}$ | $1.13 \cdot 10^{-4}$[m$^2$] |
| $c_f$ | $10 \cdot 3600$ [s/h] |
| $Cp$ | 4018 [J/(kg °C)] |
| $H$ | 79.17 [J/(s °C)] |
| $Leq$ | 46.6 [m] |
| $\beta$ | 0.432 [m] |
| $\rho$ | 1000 [kg/m$^3$] |

### *3.1 MPC Linear with feedforward action*

First, to obtain the linear model for the MPC controller, it is important to define the specific operating point, which will be applied in (4). The actual system operates in a range where the HTF flow varies from 3m$^3$/h to 15m$^3$/h, and the difference between the HTF inlet and outlet temperature varies from 2 °C to 14 °C. Hence, the operating point chosen is the desired ideal condition, in which the HTF flow of $\overline{q}$ = 14 m$^3$/h and the difference between $\overline{T}_{sc,o} - \overline{T}_{in}$ = 14 °C, considering a high irradiance situation that requires high HTF flow. Moreover, from the actual validated data, the input delay is identified as $d_q$ = 40 s. Therefore, the obtained transfer function is

$$G(s) = \left[-\frac{4.17e^{-40s}}{56.50s+1} \;\; \frac{0.053}{56.50s+1} \;\; \frac{0.211}{56.50s+1} \;\; \frac{0.788}{56.50s+1}\right], \tag{5}$$

in which $K_q$ = -4.17, $K_I$ =0.053, $K_{Ta}$ = 0.211, $K_{T_{in}}$ = 0.788, and the process time constant $\tau$ = 56.50 s.

In this representation, it is possible to describe the system's dynamics in a simplified manner through the state-space model. By employing the Zero-order hold (Zoh) discretization method and a sample time $T_s$ = 1 s, the discretized transfer functions is obtained as

$$G(z) = \left[\frac{z^{-40}(-0.07316)}{z-0.9825} \;\; \frac{0.0009298}{z-0.9825} \;\; \frac{0.003702}{z-0.9825} \;\; \frac{0.01382}{z-0.9825}\right] \tag{6}$$

The proposed discrete transfer function is used to formulate the discrete state-space representation in the form of

$$\begin{aligned}x(k+1) &= A \cdot x(k) + B_u \cdot u(k) + B_d \cdot d(k) \\ y(k) &= C \cdot x(k)\end{aligned} \quad . \tag{7}$$

Considering the SCF variables, matrix $A \in \mathbb{R}^{4\times4}$ is the state transition matrix, $B \in \mathbb{R}^{4\times1}$ is the input matrix, $B_d \in \mathbb{R}^{3\times4}$ is the disturbance matrix, and $C \in \mathbb{R}^{1\times4}$ is the output matrix. Moreover, $x$ are the system's original states, obtained directly from the discretized transfer function parameters, $u$ is the HTF flow rate $\check{q}(t)$, $d$ is the disturbances variable vector $\check{I}(t)$, $\check{T}_a(t)$, and $\check{T}_{in}(t)$, and $y(t)$ is the HTF outlet temperature $\check{T}_{sc,o}(t)$.

To eliminate the steady-state error due to the model mismatch and unmeasured disturbance, the incremental form of the inputs is implemented. These solutions allow the inclusion of an artificial state with a pole in the unitary circle that guarantees that the states are only in equilibrium when the output achieves the reference. Hence, by extending the states to include the inputs and disturbances incremental form, the extended state-space representation is developed as

$$\begin{aligned}\begin{bmatrix}x(k+1)\\u(k)\\d(k)\end{bmatrix} &= \begin{bmatrix}A & B_u & B_d\\0 & I_{nu} & 0\\0 & 0 & I_{nd}\end{bmatrix}\begin{bmatrix}x(k)\\u(k-1)\\d(k-1)\end{bmatrix} \\ &+ \begin{bmatrix}B_u\\I_{nu}\\0\end{bmatrix}\Delta u(k) + \begin{bmatrix}B_d\\0\\I_{nd}\end{bmatrix}\Delta d(k), \\ y(k) &= [C \;\; 0 \;\; 0]\begin{bmatrix}x(k)\\u(k-1)\\d(k-1)\end{bmatrix},\end{aligned} \tag{8}$$

in which $I_{nu}$ and $I_{nd}$ are the identity matrix of proper dimensions for the inputs ($nu = 1$) and the disturbances ($nd = 3$).

According to this formulation, it is possible to define the prediction calculation and, thus, the objective function, seeking to minimize the error in relation to the reference and the control effort:

Minimize:

$$J_{MPC} = \sum_{j=1}^{p} ||y(k+j|k) - y_{sp}||^2_{Q_{MPC}} + \sum_{j=0}^{m-1} ||\Delta u(k+j|k)||^2_{R_{MPC}} \quad (9)$$

Subject to (8):

$$\begin{aligned} &\Delta u(k+j|k) = u(k+j|k) - u(k+j-1|k) \\ &\Delta u_{\min} \leq \Delta U \leq \Delta u_{\max} \\ &y_{\min} \leq y \leq y_{\max} \end{aligned} \quad (10)$$

in which $p$ is the prediction horizon, $m$ is the control horizon, $Q_{MPC}$ is a positive semi-definite weight matrix for the reference tracking, and $R_{MPC}$ is a positive semi-definite weight matrix for input increments effort.

### *3.2 Nonlinear MPC*

To formulate the NMPC, the output prediction is performed using the nonlinear model of the system instead of the linear approximation as the MPC designed in Section 3.1. Therefore, the optimization problem is nonlinear, which involves a considerably more complex algorithm to solve it, resulting in a higher computational burden. Although this solution presents this meaningful drawback, the nonlinear output prediction approximates more from the actual system behavior, which can provide improved performance of the NMPC in distinct operation points. The nonlinear algorithm is applied to the model described in Section 2 according to the same objective function as the Linear MPC, such as

$$J_{NMPC} = \sum_{j=1}^{p} ||T_{sc,o}(k+j|k) - y_{sp}||^2_{Q_{NMPC}} + \sum_{j=0}^{m-1} ||\Delta u(k+j|k)||^2_{R_{NMPC}} \quad (11)$$

Subject to (1) discretized in $T_s$:

$$\begin{aligned} &\Delta u(k+j|k) = u(k+j|k) - u(k+j-1|k) \\ &u_{\min} \leq u \leq u_{\max} \\ &\Delta u_{\min} \leq \Delta u \leq \Delta u_{\max} \\ &y_{\min} \leq y \leq y_{\max} \end{aligned} \quad (12)$$

and subject to the same system constraints. In this work, a code for a nonlinear model predictive control (NMPC) will be implemented in the Matlab software using the fmincon function. From these two formulations, it will be possible to compare the efficiency of the strategies in the model.

## 4. RESULTS AND DISCUSSION

According to the controllers' formulation in Section 3, the MPC and NMPC strategies were simulated in Matlab software on a computer with technical specifications Intel Core i5 processor of 1.60GHz and 2.10 GHz and 8GB of RAM memory. The controllers were implemented under two different climate scenarios, sunny and cloudy day conditions. Moreover, the SAE (Sum of Absolute Errors) and SIC (Sum of Control Increments) indices are used to evaluate the effectiveness and performance of each controller.

The first stage of this study is to evaluate the effectiveness of the NMPC with regard to the high computational cost. Hence, a comparison concerning the sampling and processing time of each controller is developed. The strategies were subjected to the same prediction and control horizons, in addition to taking into account the slower time constant of the system due to the delay in the process, in this case, $\tau = 56.50$ s, at the operating point with this linearization constant. Therefore, the prediction horizon is given by $p \approx ((56.50 \cdot 4)/Ts)$ , and the control horizon is given by $m \approx (56.50 \cdot 40.5/Ts)$, both integer. Note that the delay $d_q$ is also considered for the simulations, using its experimentally validated nominal value, $d_q = 40$ s. The parameters of the weight matrix for the cost function were defined based on the initial conditions, using a step reference and observing overshoot, settling time and rise time. Since the process seeks a fast response to reject disturbances, the parameters were adjusted for an agile demand, despite possible oscillations, without compromising performance. For a smoother and slower control action, seeking to compensate for delays and minimize excessive oscillations, the input weights should be larger. The weights were implemented for both strategies $Q_{MPC} = Q_{NMPC} = 1e0diag(m)$, $R_{MPC} = R_{NMPC} = 1e3diag(m)$ and both scenarios for a better comparative result of responses to disturbances.

Table 2 presents the results of this analysis, where it was necessary to increase the NMPC sampling time to $T_s$=3s to obtain feasible computation. Moreover, as observed in Table 2, the MPC Linear+FF can compute the control actions with lower computational cost, with $T_s = 1$s.

Table 2. MPC Linear+FF x NMPC Processing Time

| Sampling Time | MPC Linear+FF | NMPC |
|---|---|---|
| $T_s$=1s | 0.554s | 2.5995s |
| $T_s$=2s | — | 2.3995s |
| $T_s$=3s | — | 0.7904s |

### *4.1 Sunny day scenario*

The initial conditions of the system variables for the sunny scenario were set at $q = 11.99$ m$^3$/h, $I = 486.66$ W/m$^2$, $T_a = 26.27$ °C, $T_{in} = 65.02$ °C and $T_{out} = 67.43$ °C, and both control strategies were applied under the same constraints, for input $u_{max} = 15$ m$^3$/h, $u_{min} = 3$ m$^3$/ h and $\Delta u_{max}$ = -$\Delta u_{min}$ = 1 m$^3$/h, corresponding for the actual constraints of the CIESOL facility. In the first experiment, the meteorological conditions and the HTF inlet temperature used for simulation are detailed in Figure 2.

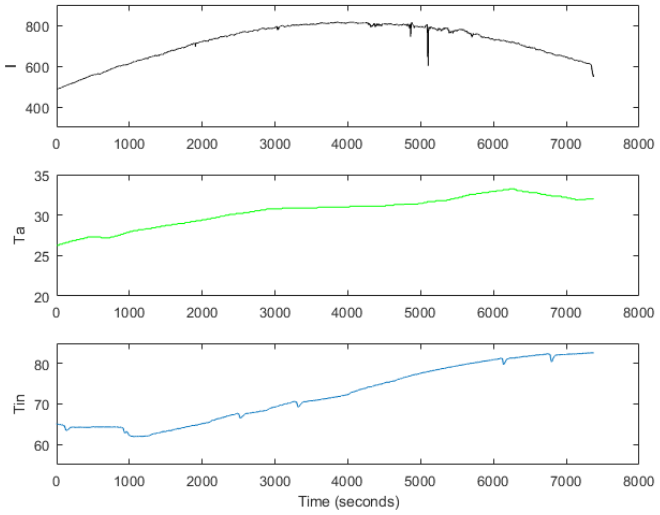


Figure 2. Input data from unmanipulated disturbances for the sunny day scenario

The linear MPC with $T_s$=1s and NMPC $T_s$=3s are employed to control the nonlinear validated model of the CIESOL SCF detailed in (1). Figure 3 depicts the controllers' performance, in which the linear strategy presents a slower response compared to the NMPC. The NMPC presented overshoot, especially under low irradiance at the beginning of the experiment. Despite minimal differences in the SAE and SIC indices detailed in Table 3, the NMPC demonstrated lower control effort, reflected in the SCI index, due to the longer sampling time. Although it maintained an effective response on sunny days, the NMPC requires higher computational cost and more robust hardware, which implies higher implementation costs, despite its superior tracking performance.

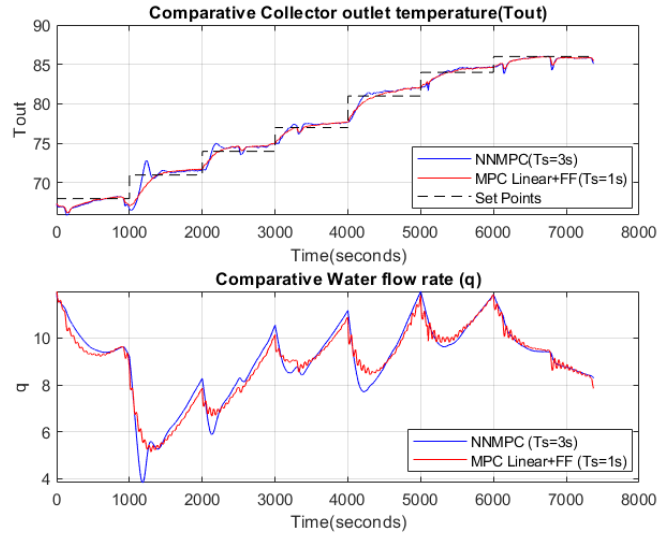


Figure 3. Comparative MPC linear+FF $T_s$=1s x NMPC $T_s$=3s

Table 3. SAE and SIC (MPC $T_s$=1s x NMPC $T_s$=3s) for the sunny day scenario

| SAE (mean error) | | SIC (sum of increments) | |
|---|---|---|---|
| MPC | NMPC | MPC | NMPC |
| 62314.4845 | 61893.4509 | 59.4997 | 42.2708 |

### *4.2 Cloudy day scenario*

In the cloudy scenario, the initial conditions of the system variables were set at $q$=12.12 m$^3$/h, $I$=749.3 W/m$^2$, $T_a$= 29.86°C , $T_{in}$ = 65.10°C and $T_{out}$ = 70.06°C, both strategies subject to the same restrictions for the input q(flow) $u_{max}$ = 15m$^3$/ h, $u_{min}$ = 3 m$^3$/ h and $\Delta u_{min}$ = -$\Delta u_{max}$ = 1 m$^3$/h. In this scenario, the input variables used to emulate the SCF field system are depicted in Figure 4.

Figure 5 presents the controllers' performance for the cloudy day experiment. As can be noted, the controllers require much more effort to regulate the HTF outlet temperature due to the effect of the passing clouds on the irradiance levels.In this test, linear MPC performed slightly better than NMPC, especially in the SCI index, where MPC performed more control actions. Sampling time is crucial: shorter times help reject frequent disturbances, but require greater effort from the manipulated variable. MPC's efficiency in adapting to rapid changes makes it more advantageous than NMPC in scenarios that require responsive control with less computational effort. NMPC presented only 2% more error than linear MPC, indicating that the longer sampling time did not significantly compromise control performance. The choice between MPC and NMPC should take into account both tracking performance and the total implementation cost, including computational demand and hardware required, in addition to expenses related to control efforts.

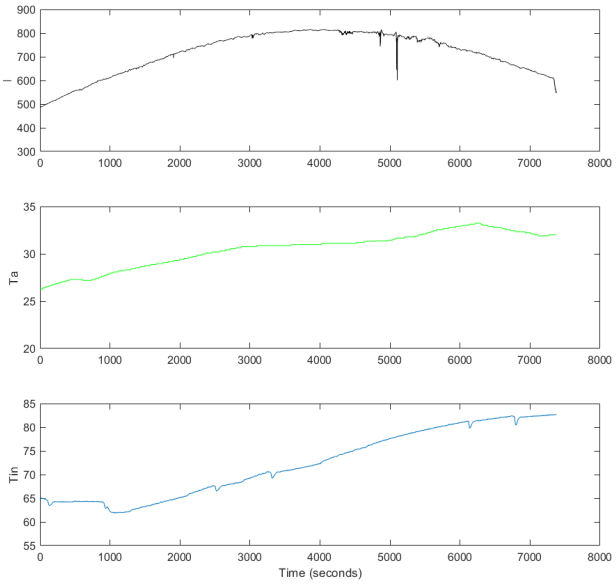


Figure 4. Input data from unmanipulated disturbances in the cloudy day scenario

Table 4. SAE and SIC (MPC $T_s$=1s x NMPC $T_s$=3s)

| SAE (mean error) | | SIC (sum of increments) | |
|---|---|---|---|
| MPC | NMPC | MPC | NMPC |
| 21887.7156 | 22508.6714 | 93.2118 | 29.0144 |

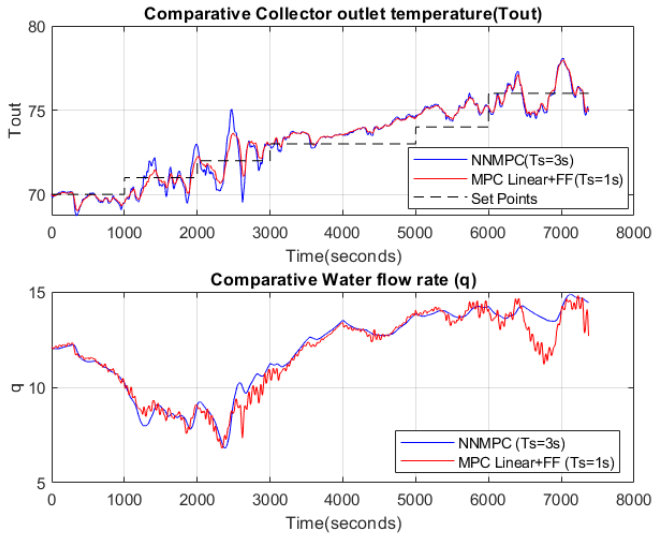


Figure 5. Comparative MPC linear+FF $T_s$=1s x NMPC $T_s$=3s

## 5. FINAL CONSIDERATIONS

The work presented a comparison presented in relation to the MPC, and NMPC applied to SCFs. The controllers are compared using actual data and a validated nonlinear model of the actual solar thermal plant facility. The simulation results demonstrated that the feasibility of the NMPC is mainly influenced by the sample time used to discretized the nonlinear model and compute the optimal control actions. Notably, the NMPC required solving a nonlinear optimization problem, which increases the computational cost and requires additional processing time. Hence, for the proposed simulation experiments, the NMPC controller increased its sampling time to 3 s, in comparison to the 1 s of the MPC.

As observed in the performance metrics, the additional sample time did not affect the NMPC's effectiveness in the sunny day scenario. The NMPC maintained a better performance in tracking references than the MPC. However, for a cloudy day scenario, the MPC controller is able to surpass the NMPC performance due to its smaller sample time that allows for rejecting faster high-frequency disturbance in the solar irradiance. It is an important comparison for some decision making and/or controller implementation considering the computational performance of the hardware.

In conclusion, when comparing these strategies under the given conditions, NMPC emerges as the more efficient option, a finding consistent with several studies in the literature. It also highlights the case that for locations that have large variations in climatic conditions and, in particular, in irradiance, the NMPC can be a more viable alternative if the control effort is translated into greater economic costs. This work provides valuable insights into the need to invest in hardware or research to increase the applicability of NMPC, even when it is necessary to increase the sampling time, despite possible compromises on cloudy days. It is essential to analyze the computational costs of NMPC when applying it to other practical systems such as SFCs, especially in systems with high-frequency disturbances, to better define the applicability limits of each approach. Future research can explore NMPC controllers with optimization techniques to balance tracking and computational efficiency. Hybrid strategies combining MPC for unstable scenarios and NMPC for more stable situations can also be investigated, aiming at better performance and lower cost.

## ACKNOWLEDGMENT

The authors would like to thank National Council for Scientific and Technological Development - CNPq - Brazil (PhD Program Abroad/ Process n$^o$ 201143/2019-4 and n$^o$ 200291/2023-8) for financial support. This work also has been funded by the National R+D+i Plan Project COMMIT4.0EB (PID2021-126889OB-I00) of the Spanish Ministry of Science and Innovation and EIE funds.

## REFERENCES

Camacho, E.F. and Bordons, C. (2017). *Model Predictive Control*. Springer-Verdag, London, England.

Camacho, E.F., Rubio, F.R., Berenguel, M., and Valenzuela, L. (2007). A survey on control schemes for distributed solar collector fields. part ii: Advanced control approaches. *Solar Energy*, 81, 1252–1272.

Camacho, E.F., Soria, M.B., Rubio, F.R., and Martínez, D. (2012). *Control of Solar Energy Systems*. Advances in Industrial Control. Springer-Verlag London.

Gallego, A.J., Sánchez, A.J., Escaño, J., and Camacho, E.F. (2022). Nonlinear model predictive control for thermal balance in solar trough plants. *European Journal of Control*, 67, 214–226.

Lemos, J.M. (2006). Adaptive control of distributed collector solar fields. *International Journal of Systems Science*, 37(8), 523–533. doi:10.1080/00207720600783686.

Li, C., Lyu, Y., Li, C., and Q, Z. (2020). Energy performance of water flow window as solar collector and cooling terminal under adaptive control. 59, 102–152.

Masero, E., Maestre, J.M., and Camacho, E.F. (2022). Market-based clustering of model predictive controllers for maximizing collected energy by parabolic-trough solar collector fields. *Applied Energy*, 306, 117936. doi: 10.1016/j.apenergy.2021.117936.

Navas, S.J., Rubio, F.R., Ollero, P., and Lemos, J.M. (2018). Optimal control applied to distributed solar collector fields with partial radiation. 159, 811–819.

Pataro, I.M.L., Gil, J.D., Americano da Costa, M.V., L., G.J., and M., B. (2021). Desarrollo de un controlador predictivo con compensación por adelanto y garantia de estabilidad: Resultados preliminares. 42, 294–300. doi: https://doi.org/10.17979/spudc.9788497498043.294.

Pataro, I.M., Gil, J.D., Americano da Costa, M.V., Guzmán, J.L., and Berenguel, M. (2022). A stabilizing predictive controller with implicit feedforward compensation for stable and time-delayed systems. *Journal of Process Control*, 115, 12–26.

Pintaldi, S., Li, J., Sethuvenkatraman, S., White, S., and Rosengarten, G. (2019). Model predictive control of a high efficiency solar thermal cooling system with thermal storage. *Energy & Buildings*, 196, 214–226.

Renewables Systems, I.E.A. (2024). International energy agency. URL `http://www.iea.org`. [Online; acesso em 19 de janeiro de 2024].